Emotion recognition and its relation to prefrontal function and network in heroin plus nicotine dependence: a pilot study

Hada Fong-ha Ieong
Zhen Yuan

SPIE.

Emotion recognition and its relation to prefrontal function and network in heroin plus nicotine dependence: a pilot study

Hada Fong-ha Ieong and Zhen Yuan*
University of Macau, Bioimaging Core, Faculty of Health Sciences, Macau SAR, China

Abstract. Many patients with substance use disorders (SUDs) live in a stressful environment, and comorbidity is not uncommon. Understanding the neural mechanisms underlying heroin and nicotine dependences and their relationships to social cognition could facilitate behavioral therapy efficacy. We aimed to provide a translational approach that leads to identifying potential biomarkers for opioid use disorder (OUD) susceptibility during recovery. We examined the clinical characters and the relationships between theory of mind (ToM) and executive functions in three groups: heroin plus nicotine-dependent (HND) patients who had remained heroin abstinent ($\geq$3 months), nicotine-dependent (ND) subjects, and healthy controls (C). The domains included emotion recognition, inhibition, shifting, updating, access, and processing speed. Resting-state functional connectivity (rsFC), ToM task-induced functional connectivity, and brain networks were then explored among 21 matched subjects using functional near-infrared spectroscopy. HND enhanced the severities of anxiety, depression, and hyperactivity. Inhibition domain was impaired in both HND and ND. No impairment in domains of emotion recognition, access, and update was observed. HND demonstrated enhanced rsFC in the medial prefrontal cortex and orbitofrontal cortex (OFC) and decreased ToM-induced connectivity across the PFC. The right superior frontal gyrus in the OFC (oSFG; $x = 22$, $y = 77$, and $z = 6$) was associated with working memory and emotion recognition in HND. Using a neuroimaging tool, these results supported the prominent reward-deficit-and-stress-surfeit hypothesis in SUDs, especially OUD, after protracted withdrawal. This may provide an insight in identifying potential biomarkers related to a dynamic environment. © *2018 Society of Photo-Optical Instrumentation Engineers (SPIE)*
[DOI: 10.1117/1.NPh.5.2.025011]

Keywords: opiate addiction; functional near-infrared spectroscopy; graph theory; resting-state functional connectivity; tobacco; translational medicine.

Paper 17128R received Nov. 10, 2017; accepted for publication May 11, 2018; published online Jun. 9, 2018.

1 Introduction

Opioid use disorder (OUD) is characterized by the compulsive opioid seeking and taking behaviors despite of its harmful consequences. Data showed 97.2% prevalence of nicotine smokers among heroin-dependent individuals.[1] From initial voluntary to habitual compulsive drug intake, the transitions involve neuroadaptations in two pathways: the dopaminergic and the glutamatergic pathways mediating the prefrontal cortex (PFC) and the striatum systems.[2,3] PFC has been clinically a target for various psychiatric illnesses owing to its known executive functioning and strong link to the limbic reward and behavioral control regions. Indeed, neuroimaging studies have contributed to identifying regional neuroadaptations resulting from chronic exposure to drugs of abuse, including the variations over the PFC, in particular, the orbitofrontal cortex (OFC), the dorsolateral PFC (dlPFC), anterior cingulate cortex, striatum, hippocampus, and amygdala (AMY). But how do the neuroadaptations in the PFC induced by the drug *per se* differ from one another at different stages of the addiction cycle? In this study, we focused on the PFC of heroin plus nicotine dependence (HND) during abstinence.

The argument that drug chronic effects of nicotine and heroin are mediated by common mechanisms is inconsistent with the knowledge that nicotine and heroin can readily be distinguished from one another. Nicotine, through inhalation, directly acts on two pathways: (1) the nicotinic cholinergic receptors mainly on the ventral tegmental area (VTA) dopamine neurons in the brain's mesolimbic dopamine system and (2) the glutamatergic terminals innervating the dopamine cell bodies.[3,4] Both pathways result in the direct stimulation of the VTA dopamine cells.[3,4] Furthermore, animal studies have shown that nicotine self-administration is blocked by antagonists of dopamine and opioid neuropeptide[5,6] and, thus, triggers the mesolimbic dopamine and opioid neuropeptide systems in the similar neural circuitry allied with other drugs of abuse.[3]

On the other hand, heroin through intravenous injection, just as other opiates, such as morphine, is analgesic and sedative owing to its actions on two pathways: (1) the mu-opioid receptors on the inhibitory GABAergic interneurons in the VTA indirectly and (2) the nucleus accumbens (NAc) neurons directly.[3] Both inhibitory pathways lead to the indirect activation of VTA dopamine neurons.[3] New evidence suggests that the endocannabinoid system, modulated by early experience and the environment, also plays a pivotal role in regulating reward-seeking behaviors and motivation processing,[7,8] which recapitulates the neuroadaptation in the opioid and dopaminergic systems.

The interplay between their mechanisms within a dynamic social environment may therefore provide insight into adaptation properties in chronic HND during recovery. Indeed, neuropsychological evidence[9] for the cognitive and behavioral adaptations suggests impairment in working memory (WM)[10] and impulsivity[11,12] while improvement in matrix reasoning and digital spin[13] after protracted abstinence. However, these studies have not fully addressed social cognition, in which its theory highlights that cognitive processes play an essential role in social interactions.[14,15]

There has been growing literature attempting to address the relationship between social cognition and executive functions (EF) in neurology.[16] Social neuroscientists suggest that theory of mind (ToM), an important component in social cognition to examine emotion recognition, may be a delineated cognitive process, separated from the general intellectual operating and other cognitive domains.[16] It is noted that human brain regions are not only segregated but also integrated,[17] constructing neural networks to harvest individual perception, cognition, and behavior, through learning[18] and the environment.[14,15,19] Few studies have examined the chronic effect of opiate use on emotion recognition,[20] and findings are inconsistent. Preliminary studies showed poor facial emotional recognition[21] and social perception deficits[22] in abstinent heroin addicts. However, another study showed no impairment but low social–emotional intelligence.[23] One highlighted the impairment in methadone-use subjects.[24] Though, conventional observations describe heroin addicts as "hustlers," that is, having the skills to mentally process one's emotion or thoughts in order to obtain funds or opiates from people through manipulation and dealing.[25] Such gaps between the neuropsychological studies and real-life observations need to be reconciled in order to understand the fundamental neural mechanisms underlying OUD within an environment where social interactions are essential for survival[19] as well as in long-term recovery.

Considering innovative psychiatric and translational study is often constrained by numerous factors,[26] the main goal of this cost-efficient study with a small sample size was to provide preliminary evidence to explore the chronic effect of heroin on cognition, producing projected scientific value for future large studies that aim to develop potential biomarkers for OUD during recovery. We examined emotion recognition, executive functions (EF), and clinical patterns using neuropsychological tests. Based on previous reports in neuroimaging and neuropsychology,[9] cognitive and emotion dysregulations are interrupted in the PFC in addiction,[2] and medial prefrontal cortex (mPFC) is one key region that governs emotion recognition.[27,28] Furthermore, we explored the functional connectivity (FC) and network in the PFC, including the mPFC, OFC, and dlPFC, at rest and when exposed to a ToM task using functional near-infrared spectroscopy (fNIRS), a rapid growing neuroimaging technique in psychiatry[29] and neurology.[30] Relationships between behavioral data and network properties were also investigated. We hypothesized that HND would demonstrate distinct patterns.

2 Materials and Methods

2.1 Participants

Thirteen HND were recruited from a local drug rehabilitation center in Macau SAR. Seven active nicotine-dependent (ND) subjects matched with the HNDs (i.e., age, education level, years of smoking, and daily cigarette consumption) were enrolled from the local community. The HND and ND were diagnosed with substance use disorders (SUDs) (i.e., OUD and tobacco use disorder (TUD), respectively) based on the diagnostic and statistical manual of mental disorders - 4th edition (DSM-IV) diagnostic criteria by clinicians. HND were enrolled based on their abstinence for at least 3 months in order to eliminate the effects of acute heroin withdrawal. Total 110 healthy control subjects (C) were recruited from the University of Macau campus via online and social media advertisement. All subjects participating in the neuropsychological assessment were urine-drug screened. Seven HND were able to proceed with the study, and thus, 7 matched C and ND were selected independently for the neuroimaging recording. The inclusion criteria of all subjects were aged between 18 and 65 years, right-handed, Cantonese speakers, and had normal or corrected-to-normal vision. The exclusion criteria were a history of neurological illness, brain surgery, other psychiatric conditions, or reported use of psychoactive substances (except methadone and nicotine) at least 72 h before assessment. Total 21 matched and included subjects were proceeded to neuroimaging assessment. The enrollment scheme of this study is shown in Fig. 1. The study was conducted in accordance with the Declaration of Helsinki of 1975. The protocol was approved by the Medical Ethics Committee of the University of Macau. All subjects provided written informed consent before participating and were compensated upon completion of the experiment.

Additional details regarding the methods and materials in this study are available in Appendix A. It includes supplementary information about the medications status of the participants, the image preprocessing and its analysis, and the FC network analyses mentioned in the main text below.

2.2 Neuropsychological Assessment

The neuropsychological battery in the study was designed to assess the EF, ToM, and behavioral stressors of the subjects. The neuropsychological domains, functions, and test administrated are tabled in Appendix B (Table 7).

EF refers to a set of abilities to carry out goal-directed behaviors, which were assessed in five domains in this study: inhibition, shifting, updating, access, and processing speed (PS). The administrated tests include stroop (STP),[9] block design (BD),[10] WM,[10,11] verbal fluency (VF),[12] and PS[10] tasks.

ToM refers to the ability to perceive and attribute mental states, including intentions and emotions to both self and others[31] and social intelligence,[32] and it was assessed in the emotion-recognition domain by the Reading the Mind in the Eyes (RME) test.[31] RME is an advanced ToM test that involves mapping mental-state lexicon and its semantics to fragments of facial expressions of mental states of others (i.e., only the part of the face around the eyes of another person). Considering cross-culture variation, the Asian RME task, which was adopted from Adams et al.,[33] was translated into Chinese from Japanese, and the Chinese version of the ToM test was piloted on a nonclinical sample of 110 healthy subjects to ensure each stimulus reached criterion level of consensus. The RME scores and the averaged reaction time of the participants are measured.

The stressors were assessed in four domains: childhood stress, depression, anxiety, and hyperactivity. The neuropsychological tests for assessing stressors include adverse childhood experiences (ACE) questionnaire,[14] Beck depression inventory-II
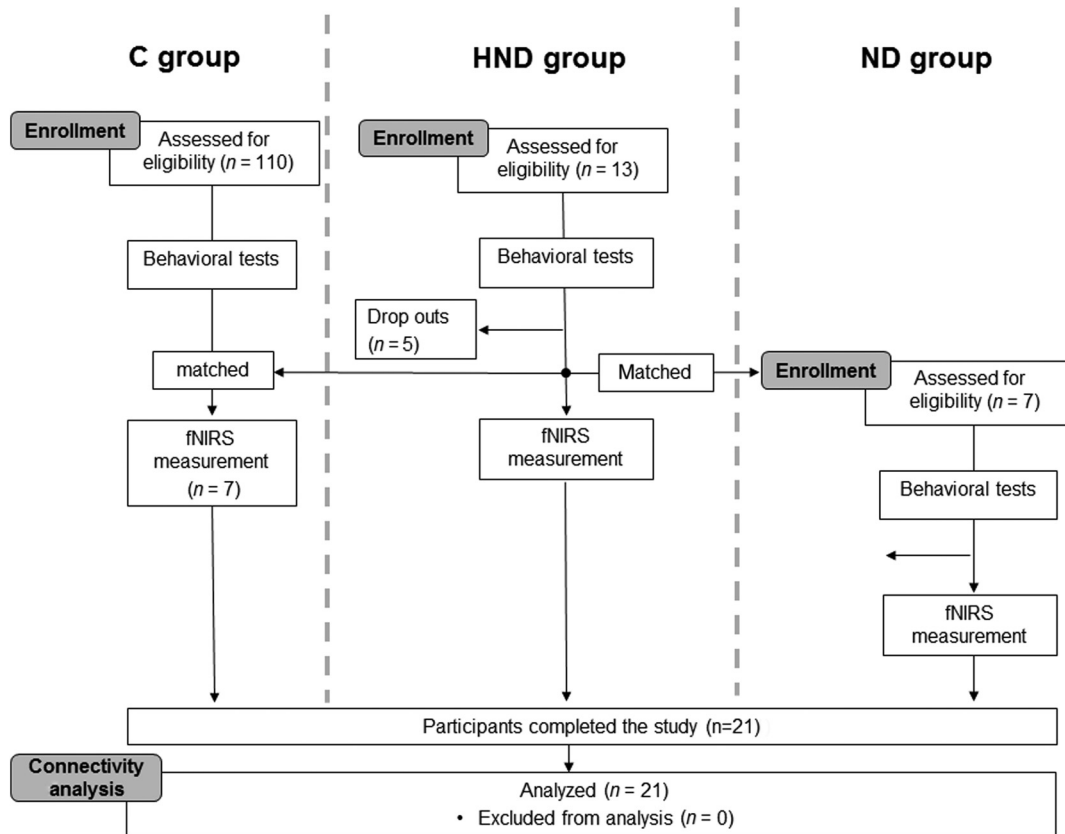
Fig. 1 Scheme of study enrollment, grouping, and evaluable participants for neuropsychological and neuroimaging measurements. The inclusion criteria of all subjects were between 18 and 65 years of age, right-handed, Cantonese speakers, and had normal or corrected-to-normal vision. The exclusion criteria were a history of neurological illness, brain surgery, other psychiatric conditions, or reported use of psychoactive substances (except methadone and nicotine) at least 72 h before assessment. A non-clinical sample of 110 healthy subjects was enrolled to ensure each stimulus in cross-cultural task reached criterion level of consensus. Total 21 matched and included subjects were proceeded to neuro-imaging assessment. The demography of the enrolled subjects is in Table 1.

(BDI-II),[15] state-trait anxiety inventory (STAI),[16] and adult attention deficit/hyperactivity disorder self-report (ASRS-v1.1) symptom checklist.[17] All enrolled subjects were required to complete a neuropsychological assessment performed by a trained psychological counselor.

2.3 Image Acquisition

All fNIRS examinations were conducted on a continuous-wave (CW) instrument (CW fNIRS system; TechEn Inc. Milford, Massachusetts) with 4 sources and 8 detectors, generating 14 channels. The regions of interest (ROIs) included the bilateral OFC, dlPFC, and mPFC. The configuration of fNIRS sources and detectors covering the PFC is shown in Fig. 2. Two CW lights at wavelengths of 690 and 830 nm were emitted during recording to detect the neurophysiological hemodynamic signals, that is, the changes in oxyhemoglobin (HbO) and in deoxyhemoglobin (Hb) in blood vessels[36] over the PFC. The sampling rate was 50 Hz. A three-dimensional (3-D) digitizer (Polhemus Inc., Vermont) was used to complete the spatial registration of the channel locations, and thus, the Montreal Neurological Institute (MNI) coordinates were obtained (Appendix C, Table 8).

Subjects were instructed to sit comfortably in a quiet dim room and move as little as possible during recordings. An 11-min, eye-closed, resting-state recording was followed by an ~11-min, eye-open, Asian RME ToM task adopted from Adams et al.[33] Resting-state and RME tasks were coded using E-prime 2.0 software (Psychology Software Tools, Inc., Pennsylvania). Before the RME task began, subjects were instructed to place their four fingers: index, middle, ring, and little fingers, on a four-button keyboard numbered from 1 to 4, respectively. Subjects were told that a pair of eyes in a picture would be displayed at the center of the screen for 3 s. During the 3 s, the subject's task was to try best to think about the emotion of the protagonist in the picture. At the fourth second, four-numbered labels of emotion were then displayed at each corner of the picture while the picture remaining at the center, and the subject's task was to choose a label that best described the emotion of the protagonist as fast and accurately as they could by pressing a corresponding button on the keyboard. Once the subject pressed the button, a fixation would be displayed for 15 s until the next stimulus was started; total 36 stimuli. The response time (RME_RT) of each stimulus was recorded in microseconds for analysis. An example of an RME stimulus is in Fig. 3.

Nodes and edges are fundamental elements of a network. In this study, nodes were defined by channels, whereas edges were defined as FC among nodes. The fNIRS-based image preprocessing for the FC generation was previously discussed in our work.[37] The HbO data were analyzed in the study due to its high sensitivity. For the task data, the time course during
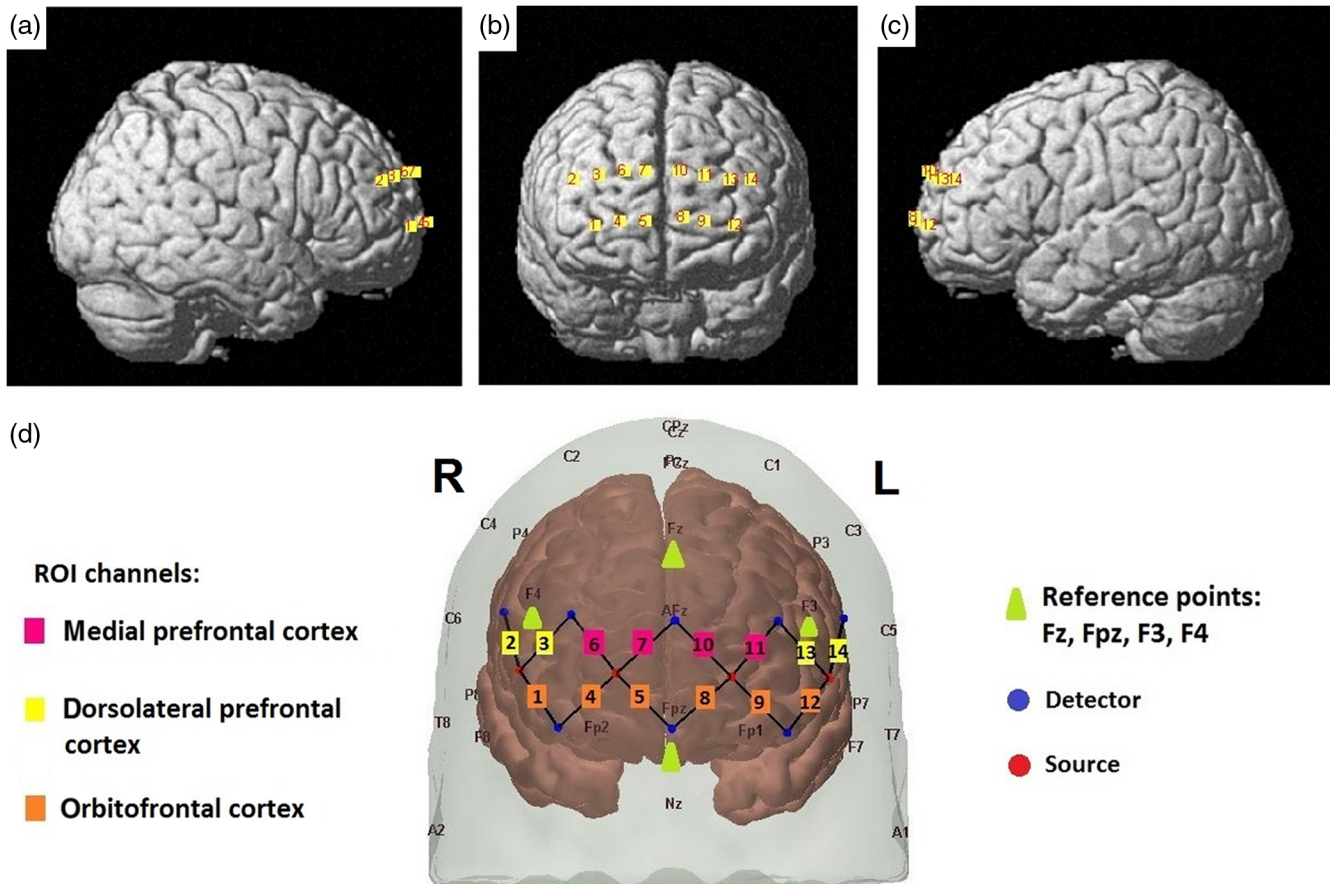
Fig. 2 Summary of 6 ROIs and their associated channels with the arrangement of the 14 channels covering the prefrontal regions. Each source and detector was 3 cm apart: (a)–(c) were generated using NIRS-SPM software[34] and (d) generated using AtlasViewer software from Homer2.[35]

Fig. 3 An example stimulus of the Asian RME for the fNIRS recording. In 1 trial, an RME stimulus was displayed at the center of the screen for 3 s when a subject's task was to read the picture and try to think about the emotion of the protagonist. Four numbered adjectives of emotion were then displayed at each corner of the picture at the fourth second, in which the subject's task was to choose an adjective that best describes the emotion at subject's fastest effort. The goal of the RME test was to assess the subject's ability to mentalize feeling and thought of others. The Asian RME was adopted from Adams,[33] and the labels were translated in Chinese as the figure shown from Japanese. Language in English, Chinese, and Japanese as follow: (1) embarrassed, 尷尬, きまりが悪い, (2) guilty, 內疚, 気がとがめている, (3) fantasizing: 幻想, 空想にふけっている, and (4) concerned (target), 擔心, 心配そうにしている. Reproduced with permission from Adams.[33]

the 3-s mental recording and its 17-s hemodynamic delay were extracted for analysis. Whole-brain analysis was used to test the FC strength. A mean group-level correlation matrix of each set data was obtained from the resting-state and ToM-task fNIRS data separately for each study group. The foremost 10% of connections calculated from the population (method details in Niu et al.[38]) were used as the threshold. Correlations coefficients greater than the predetermined threshold value were considered as edge. The details of the method are available in Appendix A.

2.4 Statistics

Statistical analyses were performed using SPSS (IBM SPSS Statistics, Armonk, New York). Group differences in demographic, behavioral, and ROI data were investigated using one-way ANOVA and Bonferroni correction. Using a current alternative strategy,[26,39] the matched sample size (i.e., n_{root}) was appropriately adapted to the cost concerns of the study. Prior to any statistical analysis, all correlation values were converted to Fisher z-values using the Fisher z-transformation, which has been widely used when the sample size is <30. Within-group correlations among neuropsychological measures were tested using Spearman's rank-order test. Linear regression analysis was conducted to examine any link between behavioral measures and FC patterns for each ROI. Multiple regression was performed for all significant results to account for potential differences in age, education level, and IQ. To address the

issue of multiple comparisons, Bonferroni correction was applied to the *post hoc* tests for behavioral and imaging measures.

3 Results

3.1 Demographics

Subjects' demographic characteristics and drug-taking behaviors are summarized in Table 1. Age, education, and sex were significant in the controls because most of them were recruited from our campus, but they did not differ ($p > 0.05$) between groups after matching. Seven controls and 7 ND were matched with 7 HND subjects included in the neuroimaging recording. The attempt-to-commit-suicide rates during lifetime in the dependent groups were significantly higher ($p < 0.0001$) than the controls. The smoking habitual behaviors, such as daily dose and years of smoking, did not differ between the dependent groups, but the onset age did ($p < 0.001$). HND

had a mean (SD) smoking onset at age 13.7 (2.0), whereas ND had at 17.0 (1.5).

3.2 Heroin Plus Nicotine Dependence Enhances Severity of Stressors

Both HND and ND demonstrated significantly ($p < 0.0001$) higher levels of anxiety and childhood adversity compared with the controls (Table 2). The depressive- and attention deficit/hyperactivity disorder (ADHD)-like responses were observed only in HND ($p < 0.001$). The *post hoc* tests showed that HND had a significant effect ($p < 0.01$) on the severity of hyperactivity, anxiety, and depression. Within the clinical measures (Fig. 4), the depression-like response predicted the level of anxiety in ND ($R^2 = 0.594$, $F_{1,6} = 7.31$, $p = 0.043$, $\beta = 1.59$) and hyperactivity ($R^2 = 0.743$, $F_{1,6} = 14.4$, $p = 0.013$, $\beta = 0.315$); whereas these variables were only correlated in HND ($r = 0.550$; $r = 0.118$, $p > 0.05$, respectively).

Table 1 Demographic characteristics for the studied groups.

N	C		ND	HND	Significant value[a]	
	110	7	7	13		
	Total	Matched			Total	Matched
Age (years)	28.6 (7.53)	36.6 (10.7)	45.6 (6.83)	44.6 (8.24)	<0.0001	0.11
Gender; M:F	36:74	3:4	7:0	10:3	<0.0001	0.058
Years of education	16.9 (3.29)	8.14 (2.97)	7.00 (2.66)	5.88 (2.95)	<0.0001	0.259
Estimated IQ (WAS-II)	98.4 (26.6)	79.9 (13.2)	83.1 (9.26)	84.5 (12.6)	0.064	0.719
Hours of sleeping per day	7.12 (0.90)	7.00 (0.90)	7.00 (1.52)	7.56 (0.776)	0.247	0.123
Suicide attempt; yes:no	1:109	1:6	1:6	5:8	<0.0001	<0.0001
Smoking behavior[b]						
Nicotine dependence/TUD DSM-IV	No		Yes	Yes	>0.05	
Years of smoking	n.a.		28.7 (7.30)	31.9 (8.10)	0.396	
Daily dose of nicotine (mg)[c]	n.a.		20.0 (10.7)	21.2 (9.50)	0.799	
Age of smoking onset	n.a.		17.0 (1.50)	13.7 (2.00)	0.001	
Heroin-taking behavior[b]						
Opiate dependence/OUD DSM-IV	No		No	Yes	<0.0001	
Duration of heroin use (years)	n.a.		n.a.	28.0 (9.00)	—	
Age of drug-taking onset	n.a.		n.a.	19.4 (8.10)	—	
Duration of heroin abstinent (months)	n.a.		n.a.	24.6 (38.2)	—	
Former daily dose of heroin (g)	n.a.		n.a.	3.00 (2.00)	—	
Treatment; MMT:without MMT	n.a.		n.a.	5:8	—	
Daily dose of methadone (mg)	n.a.		n.a.	33.9 (27.1)	—	

Note: Abbreviations: C, healthy control; ND, nicotine dependence; HND, heroin dependence with nicotine dependence; and n.a., not applicable.
[a]One-way ANOVA, or χ^2 test, or two-sample *t*-test for the *p*-values between or within groups.
[b]Self-reported data: Two-sample *t*-test between ND and HND.
[c]1-mg nicotine absorbed per cigarette.

Table 2 Differences between studied groups in EF, ToM, and clinical measures.

	Item	C	ND	HND	F-value	p-value	Post hoc p-value[a]		
Behaviors	N	110	7	13	One-way ANOVA	One-way ANOVA	C versus HND	C versus ND	HND versus ND
Task/test	Domain/measure								
			EF measures						
STP	Inhibition	0.314 (0.161)	−0.098 (0.365)	0.161 (0.371)	15.8	<0.0001	0.031	<0.0001	0.021
BD	Shifting	12.7 (3.33)	10.1 (2.42)	7.91 (2.47)	14.3	<0.0001	<0.0001	0.100	0.319
WM	Updating	84.9 (10.1)	82.6 (11.8)	82.5 (13.0)	0.431	0.651	0.716	0.840	0.995
VF	Access	21.0 (5.15)	16.3 (2.71)	17.9 (5.68)	4.56	0.012	0.101	0.052	0.783
PS	Processing speed	98.5 (9.96)	100.9 (12.9)	89.1 (13.1)	5.06	0.008	0.007	0.826	0.045
			ToM measures						
RME (Asian)	Emotion recognition	25.9 (3.22)	24.6 (2.87)	24.3 (4.46)	1.60	0.207	0.364	0.420	0.979
RME_RT (ms)	Emotion recognition	5439 (1041)	10337 (4375)	5526 (1532)	38.7	<0.0001	0.977	<0.0001	<0.0001
			Clinical characteristic and mood measures						
ADHD	Hyperactivity	1.73 (0.770)	2.00 (1.85)	5.27 (1.86)	73.4	<0.0001	<0.0001	0.767	<0.0001
STAI	Anxiety	59.0 (11.1)	74.1 (15.2)	93.5 (19.6)	48.2	<0.0001	<0.0001	0.006	0.003
BDI	Depression	10.1 (3.18)	12.0 (6.80)	21.6 (9.55)	39.7	<0.0001	<0.0001	0.512	<0.0001
ACE	Childhood stress	0.018 (0.133)	1.14 (1.12)	2.70 (2.41)[b]	71.7	<0.0001	<0.0001	0.0007	0.0001

Note: Abbreviations: C, healthy control; ND, nicotine dependence; HND, heroin dependence with nicotine dependence; STP, stroop; BD; block design; MW, working memory; VF, verbal fluency; PS, processing speed; EF, executive function; ToM, theory of mind; BDI, Beck depression inventory; STAI, state-trait anxiety inventory; ACE, adverse childhood experience; SUD DSM-IV, DSM-IV; EF, diagnostic criteria for SUDs; and n.a., not applicable. Measures are detailed in Appendix A and Appendix B (Table 7).
[a]One-way ANOVA. Tukey's *post hoc* Bonferroni corrected.
[b]$N = 12$. One subject grew up in orphanage until 18; the childhood experiences were out of the ACE measuring scope.
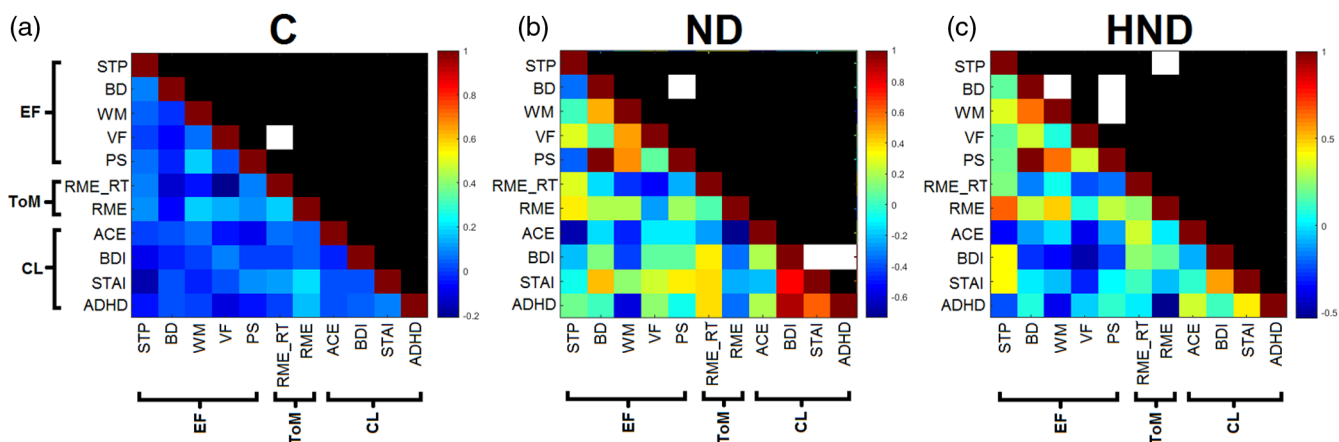

Fig. 4 Correlation matrices between neuropsychological variables: EF, ToM, and clinical characteristics. Statistically significant correlations within-group comparisons: (a) healthy controls (C), (b) ND group, and (c) HND group. Neuropsychological tests include STP, BD, WM, VF, and PS in the EF domain, and RME test and its response time (RME_RT) in the ToM domain. Clinical measurements include ACE, BDI, STAI, and the adult ADHD tests. Color bars represent the Z to R correlation coefficient values. Pearson's correlations were used. White cube represents significant correlations ($p < 0.05$) in regression. Black region represents nonsignificance in regression. The neuropsychological tests administrated in this study are detailed in Appendix B (Table 7).
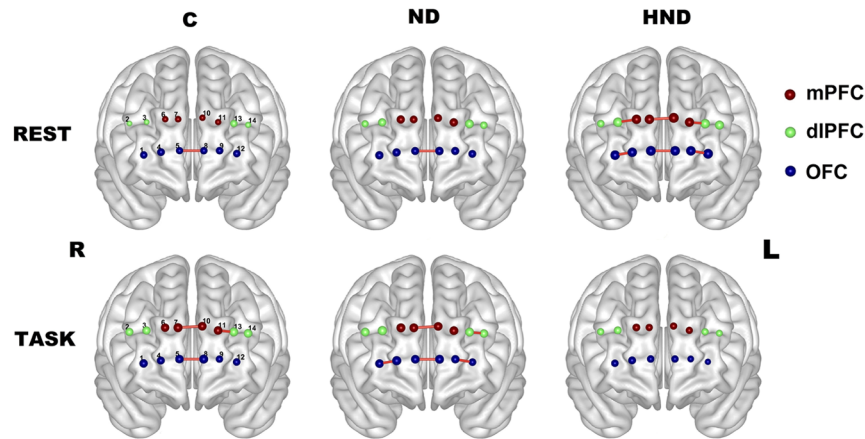
Fig. 5 Whole-brain correlation analysis for comparison of brain networks in healthy controls (C), ND, and HND groups. The top column indicates resting-state networks. The below indicates ToM-induced networks. Only the topmost 10% with correlation values greater than the predetermined thresholds (T_{rest}: 0.87 and T_{task}: 0.85) are shown in the figure. The nodes represent the channels. The edges represent the connections. The nodes (red: medial prefrontal regions, blue: orbitofrontal regions, and green: dorsolateral prefrontal regions) are numbered by channel in control group. The weighted nodes are displayed. R: right and L: left. HbO data during resting-state and ToM task are in Tables 3 and 4, respectively, whereas Hb data are in Tables 5 and 6, respectively.

Table 3 Group differences in nodal degree strength in the change of HbO concentration (ROI analysis) during resting state.

ROI	Ch	Region	C	ND	HND	F-value	p-value	Post hoc p-value[a]		
			7	7	7	One-way ANOVA	One-way ANOVA	C versus HND	C versus ND	HND versus ND
OFC_R	1	oMFG_R	0.449 (0.047)	0.534 (0.045)	0.660 (0.053)	4.80	0.0213	0.0169	0.0169	0.186
	4	oSFG_R	0.487 (0.045)	0.537 (0.055)	0.664 (0.059)	2.93	0.0793	0.0746	0.788	0.238
	5	mOFC_R	0.429 (0.057)	0.520 (0.055)	0.708 (0.060)	6.15	0.0092	0.0078	0.514	0.0789
dlPFC_R	2	MFG_R	0.244 (0.041)	0.421 (0.050)	0.464 (0.036)	7.45	0.0044	0.0051	0.0232	0.760
	3	SFG_R	0.269 (0.053)	0.532 (0.054)	0.653 (0.054)	13.4	0.0003	0.0002	0.0074	0.274
mPFC_R	6	SFG_R	0.346 (0.045)	0.542 (0.054)	0.654 (0.058)	8.78	0.0022	0.0017	0.0425	0.312
	7	mPFC_R	0.361 (0.046)	0.484 (0.051)	0.658 (0.059)	8.15	0.0030	0.0022	0.246	0.0736
OFC_L	8	mSFG_L	0.456 (0.051)	0.557 (0.054)	0.681 (0.058)	4.29	0.030	0.0234	0.407	0.267
	9	SFG_L	0.458 (0.054)	0.525 (0.053)	0.675 (0.060)	3.97	0.0372	0.0334	0.678	0.167
	12	SFG_L	0.461 (0.050)	0.497 (0.048)	0.700 (0.059)	6.01	0.010	0.0127	0.880	0.0349
mPFC_L	10	SFG_L	0.337 (0.057)	0.500 (0.052)	0.707 (0.059)	10.9	0.0008	0.0005	0.128	0.0445
	11	mSFG_L	0.327 (0.033)	0.555 (0.053)	0.643 (0.064)	9.98	0.0012	0.0011	0.0154	0.465
dlPFC_L	13	MFG_L	0.442 (0.031)	0.584 (0.049)	0.647 (0.053)	19.3	<0.0001	0.0132	<0.0001	0.0196
	14	MFG_L	0.301 (0.033)	0.444 (0.044)	0.615 (0.047)	14.2	0.0002	0.0001	0.0647	0.0249

Note: Abbreviations: C, healthy control; ND, nicotine dependence; HND, heroin dependence with nicotine dependence; ROI, region of interest; and Ch, channel.
Degree strengths along with the standard errors of the mean (SEM) in all regions with significant level of $p < 0.01$ in ANOVA are presented.
[a]Bonferroni corrected.

3.3 Relations between EF and ToM Mechanisms

The EF and ToM performances are shown in Table 2. Both HND and ND showed significantly ($p < 0.0001$) poor performance in the STP test (i.e., inhibition domain) compared with the controls. While compared with ND, HND patients showed significantly ($p = 0.021$) better performance in STP. There were significant effects of heroin dependence on the BD, and PS ($F_{2,127} = 14.3$, $p < 0.0001$, and $F_{2,127} = 5.06$, $p < 0.0001$, respectively), indicating chronic heroin consumption mediated and reduced both aspects of shifting and PS skills. A significant main effect of drug dependence ($F_{2,127} = 4.56$, $p = 0.012$) indicated that chronic drug consumption impaired the access domain but *post hoc* comparison of the ND and HND with the controls did not reach significance. No significant effects of heroin and nicotine on the updating domain were found. The longest response time of the RME task in ND compared with HND and controls was observed.

Correlation and further regression analyses were performed. The relationships between EF, ToM, and clinical characteristics of each group are shown in Fig. 4. Within the EF measures in HND, PS was significantly associated with BD (i.e., the shifting domain; $R^2 = 0.990$, $F_{1,12} = 40,529$, $p < 0.0001$, $\beta = 4.06$) and WM (i.e., the updating domain; $R^2 = 0.384$, $F_{1,12} = 5.62$, $p = 0.042$, $\beta = 0.616$), which was also linked to BD ($R^2 = 0.377$, $F_{1,12} = 5.54$, $p = 0.044$, $\beta = 2.48$). Similar to HND, ND showed a strong association between PS and the shifting domains ($R^2 = 0.998$, $F_{1,7} = 2699$, $p < 0.0001$,

$\beta = 0.999$). No significant association within the EF measures was observed in controls.

Between the EF and ToM measures, the performance of RME was associated with that of STP ($R^2 = 0.379$, $F_{1,12} = 5.50$, $p = 0.044$, $\beta = 2.45$) in HND. There was an association between VF (i.e., the access domain) and the response time of RME ($R^2 = 0.047$, $F_{1,109} = 5.38$, $p = 0.022$, $\beta = -0.001$) in controls. No significant EF–ToM association was observed in ND.

3.4 Functional Connectivity

Total 21 subjects were matched with age ($F_{2,18} = 1.46$, $p = 0.258$), education level ($F_{2,18} = 2.79$, $p = 0.088$), and estimated IQ ($F_{2,18} = 0.361$, $p = 0.702$) and were included in the neuroimaging analysis.

The resting-state correlation coefficient threshold value was 0.87 (mean = 0.52), and the task-induced correlation coefficient threshold was 0.85 (mean = 0.52). Group-level HbO-based connectivity maps during resting state and task are shown in Fig. 5. The resting-state functional connectivity (rsFC) map for HND showed consistent results from prior studies.[37,40,41] Consistent with our *a priori* hypothesis of a positive relationship between clinical stressors and OFC during resting state,[37] we discovered enhanced rsFC connectivity strength in the OFC and mPFC but decreased in dlPFC. The HbO-based nodal degree strength of each ROI from resting-state and ToM-task

Table 4 Group differences in degree strength in the change of HbO concentration (ROI analysis) during RME task.

ROI	Ch	Region	C	ND	HND	F-value	p-value	Post hoc p-value[a]		
			7	7	7	One-way ANOVA	One-way ANOVA	C versus HND	C versus ND	HND versus ND
OFC_R	1	oMFG_R	0.559 (0.024)	0.574 (0.038)	0.452 (0.042)	3.51	0.0517	0.112	0.952	0.0637
	4	oSFG_R	0.501 (0.049)	0.632 (0.030)	0.498 (0.030)	4.18	0.0323	0.998	0.0582	0.0520
	5	mOFC_R	0.560 (0.046)	0.577 (0.034)	0.452 (0.045)	2.25	0.135	0.693	0.425	0.117
dlPFC_R	2	MFG_R	0.513 (0.028)	0.579 (0.035)	0.434 (0.034)	5.00	0.0188	0.225	0.344	0.0144
	3	SFG_R	0.532 (0.050)	0.641 (0.037)	0.484 (0.037)	3.71	0.0449	0.700	0.184	0.0406
mPFC_R	6	SFG_R	0.553 (0.050)	0.609 (0.048)	0.472 (0.040)	2.22	0.137	0.446	0.673	0.119
	7	mPFC_R	0.614 (0.050)	0.597 (0.037)	0.432 (0.055)	5.28	0.0157	0.0168	0.795	0.0631
OFC_L	8	mSFG_L	0.611 (0.035)	0.601 (0.033)	0.430 (0.041)	7.77	0.0037	0.0068	0.980	0.0103
	9	SFG_L	0.432 (0.046)	0.541 (0.051)	0.377 (0.052)	2.82	0.0863	0.719	0.292	0.0768
	12	SFG_L	0.467 (0.038)	0.476 (0.053)	0.327 (0.054)	2.92	0.0797	0.135	0.991	0.107
mPFC_L	10	SFG_L	0.583 (0.055)	0.572 (0.042)	0.432 (0.058)	2.61	0.101	0.129	0.988	0.168
	11	mSFG_L	0.574 (0.046)	0.595 (0.042)	0.421 (0.046)	4.51	0.0258	0.0648	0.941	0.0334
dlPFC_L	13	MFG_L	0.612 (0.028)	0.588 (0.048)	0.413 (0.047)	6.68	0.0067	0.0095	0.914	0.0224
	14	MFG_L	0.568 (0.036)	0.556 (0.040)	0.394 (0.035)	6.78	0.0064	0.0106	0.972	0.0173

Note: Abbreviations: C, healthy control; ND, nicotine dependence; HND, heroin dependence with nicotine dependence; ROI, region of interest; and Ch, channel.
Degree strengths along with the SEM in all regions with significant level of $p < 0.01$ in ANOVA are presented.
[a]Bonferroni corrected.

Table 5 Group differences in nodal degree strength in the change of Hb concentration (ROI analysis) during resting state.

ROI	Ch	Region	C	ND	HND	*F*-value	*p*-value	*Post hoc p*-value[a]		
						One-way ANOVA	One-way ANOVA	C versus HND	C versus ND	HND versus ND
			7	7	7					
OFC_R	1	oMFG_R	0.226 (0.041)	0.286 (0.040)	0.344 (0.043)	4.24	0.0310	0.0261	0.571	0.183
	4	oSFG_R	0.067 (0.083)	0.367 (0.039)	0.438 (0.056)	10.3	0.0011	0.0014	0.0065	0.763
	5	mOFC_R	0.146 (0.074)	0.315 (0.060)	0.450 (0.065)	5.23	0.0162	0.0123	0.200	0.345
dlPFC_R	2	MFG_R	0.209 (0.053)	0.207 (0.050)	0.158 (0.040)	0.362	0.701	0.737	0.999	0.754
	3	SFG_R	0.224 (0.076)	0.331 (0.051)	0.399 (0.024)	2.61	0.101	0.0871	0.369	0.659
mPFC_R	6	SFG_R	0.236 (0.074)	0.322 (0.055)	0.403 (0.061)	1.71	0.209	0.182	0.615	0.649
	7	mPFC_R	0.059 (0.074)	0.294 (0.068)	0.373 (0.067)	5.49	0.0138	0.0136	0.0696	0.707
OFC_L	8	mSFG_L	0.185 (0.049)	0.311 (0.058)	0.438 (0.071)	4.44	0.027	0.0208	0.321	0.316
	9	SFG_L	0.208 (0.060)	0.277 (0.048)	0.441 (0.064)	4.30	0.0298	0.0271	0.681	0.139
	12	SFG_L	0.288 (0.049)	0.208 (0.047)	0.434 (0.042)	6.18	0.009	0.0913	0.453	0.0074
mPFC_L	10	SFG_L	0.078 (0.064)	0.293 (0.076)	0.477 (0.061)	8.80	0.0022	0.0015	0.0881	0.158
	11	mSFG_L	0.175 (0.070)	0.390 (0.057)	0.498 (0.058)	7.05	0.0055	0.0046	0.061	0.450
dlPFC_L	13	MFG_L	0.285 (0.040)	0.389 (0.055)	0.437 (0.040)	2.91	0.080	0.0728	0.265	0.740
	14	MFG_L	0.243 (0.051)	0.330 (0.044)	0.309 (0.040)	1.01	0.385	0.567	0.382	0.943

Note: Abbreviations: C, healthy control; ND, nicotine dependence; HND, heroin dependence with nicotine dependence; ROI, region of interest; and Ch, Channel.
Degree strengths along with the SEM in all regions with significant level of $p < 0.01$ in ANOVA are presented.
[a]Bonferroni corrected.

data is available in Tables 3 and 4, respectively, provided with *post hoc* analyses, whereas the Hb-based data are in Tables 5 and 6, respectively.

In line with evidence that mPFC plays a significant role in ToM cross cultures,[27,33] the ToM-induced connectivity maps for the healthy subjects also demonstrated similar connections within the mPFC and between the mPFC and the dlPFC regions in the left hemisphere from prior studies.[28,31] During RME, we observed decreased FC across the PFC in HND but enhanced FC in ND, including the connections between the orbital portions of middle and superior frontal gyri within the right OFC regions, between the superior frontal gyri within the left OFC, and between the left superior frontal gyri within the left dlPFC, compared with the controls.

3.5 Relations between Behavioral Performance and Network Organization

The rsFC local and global network topological properties are plotted as a function of sparsity in Fig. 6. Several correlations and multiple linear regression with *post hoc* analyses were performed with the neuropsychological performances. We observed a significant association ($R^2 = 0.756$, $F_{1,6} = 15.5$, $p < 0.01$, $\beta = 8.82$) between WM performance and nodal degree strength on the right orbital part of superior frontal gyrus (oSFG; i.e., channel 4, $x = 22$, $y = 72$, and $z = 6$) in HND [Fig. 6(f)]. At the same region, a significant association

($R^2 = 0.779$, $F_{1,6} = 17.7$, $p < 0.01$, $\beta = 13,685$) between the RME response time and clustering coefficient was also observed in HND [Fig. 6(g)].

4 Discussion

We profiled the EF and emotion recognition performances with clinical variables between HND and ND. Impairment in PS and risks of hyperactivity and depression were observed in HND, whereas longer, but not impaired, mental processing was required in ND. Emotion recognition was associated with EF inhibition in HND. Drug–drug interactions were observed. In addition to nicotine, chronic exposure to heroin downregulated the shifting and upregulated the inhibition, emotion recognition in ToM, and the anxiety-like response even during abstinence of heroin (≥ 3 months). No deficit in the updating and access domains was observed in both HND and ND. We showed that their prefrontal networks change as a function of ToM mental processing and resting. HND is characterized by the enhanced functionality strength at rest but reduced during mental task in the PFC network. ND is the reverse. The right oSFG was associated with emotion recognition globally and WM locally within the PFC network in HND. These findings have essential implications in the conceptualization of social cognition and in the path to identify potential biomarkers to treatment response as well as the improvement to behavioral therapy efficacy in OUD.

Table 6 Group differences in degree strength in the change of Hb concentration (ROI analysis) during RME task.

ROI	Ch	Region	C	ND	HND	*F*-value	*p*-value	Post hoc *p*-value[a]		
						One-way ANOVA	One-way ANOVA	C versus HND	C versus ND	HND versus ND
			7	7	7					
OFC_R	1	oMFG_R	0.306 (0.056)	0.440 (0.039)	0.278 (0.038)	3.69	0.0455	0.900	0.118	0.0512
	4	oSFG_R	0.388 (0.055)	0.472 (0.042)	0.360 (0.020)	1.96	0.169	0.883	0.348	0.166
	5	mOFC_R	0.331 (0.061)	0.388 (0.043)	0.196 (0.062)	3.10	0.0698	0.231	0.755	0.0643
dlPFC_R	2	MFG_R	0.335 (0.031)	0.408 (0.046)	0.230 (0.037)	5.40	0.0145	0.159	0.392	0.0113
	3	SFG_R	0.173 (0.063)	0.507 (0.048)	0.334 (0.039)	10.7	0.0009	0.0924	0.0006	0.0673
mPFC_R	6	SFG_R	0.176 (0.067)	0.494 (0.050)	0.250 (0.049)	8.85	0.0021	0.626	0.0022	0.0168
	7	mPFC_R	0.303 (0.064)	0.460 (0.044)	0.284 (0.044)	3.51	0.0515	0.963	0.107	0.0654
OFC_L	8	mSFG_L	0.250 (0.071)	0.391 (0.045)	0.196 (0.064)	2.72	0.0925	0.808	0.257	0.0878
	9	SFG_L	0.259 (0.060)	0.441 (0.052)	0.282 (0.044)	3.58	0.0492	0.948	0.0605	0.109
	12	SFG_L	0.325 (0.060)	0.352 (0.058)	0.226 (0.054)	1.34	0.288	0.457	0.941	0.291
mPFC_L	10	SFG_L	0.288 (0.062)	0.464 (0.047)	0.306 (0.052)	3.21	0.0641	0.970	0.081	0.125
	11	mSFG_L	0.342 (0.050)	0.492 (0.053)	0.278 (0.061)	4.01	0.0363	0.693	0.158	0.033
dlPFC_L	13	MFG_L	0.370 (0.044)	0.462 (0.060)	0.306 (0.057)	2.10	0.152	0.686	0.467	0.132
	14	MFG_L	0.130 (0.038)	0.370 (0.048)	0.237 (0.047)	7.28	0.0048	0.233	0.0035	0.116

Note: Abbreviations: C, healthy control; ND, nicotine dependence; HND, heroin dependence with nicotine dependence; ROI, region of interest; and Ch, channel.
Degree strengths along with the SEM in all regions with significant level of *p* < 0.01 in ANOVA are presented.
[a]Bonferroni corrected.

Stress exposure plays a prominent role in early development and in the disruption of the endocannabinoid-mediate plasticity in NAc, AMY, which engage in emotion regulation in addiction.[8] Consistent with prior evidence, both of the dependent groups demonstrated high level of anxiety-like responses[2,18] and stressors from ACE.[42] Depression-like responses and hyperactivity in particular were prevalent among HND. Recent compelling evidence suggests that the increased anxiety and depression are associated with the disruption of the endocannabinoid signaling, which may reflect the negative affective states and enhanced stress responses[8] that regulate the negative reinforcement mechanisms during drug withdrawal.[43] Although neither anxiety disorder nor major depression was diagnosed between HND and ND, we proposed that the acute withdrawal of nicotine may link to the anxiety-like responses, and the protracted withdrawal of heroin may link to depressive-like and hyperactive behaviors and enhance the severity of anxiety, suggesting that these aversion states could be possible predictors for OUD susceptibility.

This study showed enhanced rsFC and reduced ToM-induced FC in the PFC in HND and the reverse in ND. We believe that the discrepancy in neural activities was influenced by dynamic allocation of attentional resources depending on task demands.

At rest, the protracted withdrawal and craving of heroin in HND may reinforce two pathways: (1) between the PFC, particularly OFC, and AMY,[37,40,44] including the basolateral AMY,[45] which regulates emotion, memory, and sensory and

(2) between the OFC and hippocampus, which mediates memory.[18] Because these regions had direct projections to the PFC and OFC through acetylcholine and monoamine transmissions, *vice versa* through the glutamine, fNIRS was able to detect the cortical oxygenation signals, that is, the enhanced HbO-based rsFC manifested in the PFC of HND. In contrast, the acute withdrawal of nicotine in ND may reinforce the pathway between the AMY, the extended AMY, and ventral striatum, which mediates the stress, anxiety, and aversive systems.[43] Because most of these areas were underneath the cerebral cortex where fNIRS cannot detect the oxygenation activity, that is, the reduced rsFC manifested in ND. These drug-and-stage-specific actions in the brain reward circuits are very likely to play an important role in the stage-specific maladaptation after chronic-specific drug use. This interpretation was also in line with our findings, which recapitulates the amplified aversive systems after prolonged removal of heroin. Thus, this study adds to a growing literature that supports the reward-deficit-and-stress-surfeit (i.e., the negative reinforcement) hypothesis[2] and appeals to a current compelling interpretation that the neuro-adaptations underlying OUD during protracted abstinence involve associated memory and emotion.[18] During ToM task, the enhanced FC in ND was in line with the finding in their response duration, suggesting that significant allocation of attentional resource to the PFC during mental processing in ND. The reduced FC in HND supports the prominent hypothesis of baseline activity of PFC and OFC (i.e., hypofunctionality) as the
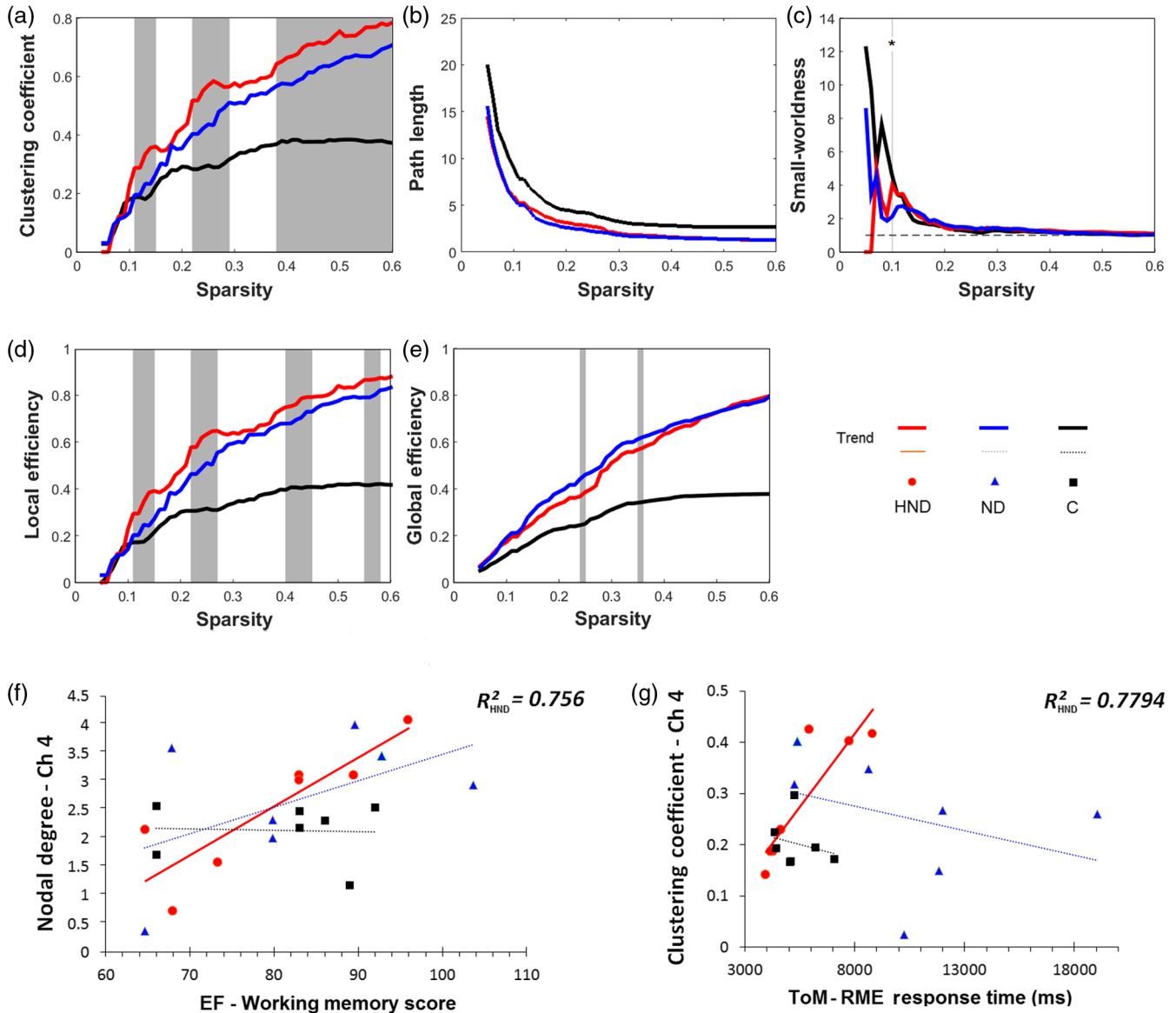
Fig. 6 Brain topological network and its relationship with cognitive functions. (a)–(e) Brain functional network properties as a function of sparsity, S, in healthy controls (C; black), ND (blue), and HND (red) groups. (a) Clustering coefficient; significant ranges: $0.11 < S < 0.15$ $(0.009 < p < 0.032)$, $0.22 < S < 0.29$ $(0.009 < p < 0.044)$, and $0.38 < S < 0.60$ $(0.009 < p < 0.030)$. (b) Characteristic path length; nonsignificance. (c) Small-worldness; significant at $S = 0.1$ $(p = 0.047)$. (d) Local efficiency; significant ranges: $0.11 < S < 0.15$; $0.22 < S < 0.27$; $0.4 < S < 0.45$; $0.55 < S < 0.58$, $0.009 < p < 0.05$. (e) Global efficiency; significant ranges: $0.24 < S < 0.25$ $(p = 0.033)$ and $0.35 < S < 0.36$ $(p = 0.037)$. (f)–(g) Regression between network property and cognitive function. (f) WM index in the EF domain versus the nodal network property, nodal degree at the right oSFG $(x = 22, y = 77, z = 6; F_{1,6} = 15.5, p = 0.013, \beta = 8.82)$. (g) RME task in the ToM versus the global network property, clustering coefficient at the right oSFG $(F_{1,6} = 17.7, p < 0.01, \beta = 13,685)$.

typical neuroadaptation after chronic opioid use. Although it is unknown to what extend the hypofunctionality relates to brain functions, our findings of the normality in emotion-recognition performance in HND and its association with inhibition suggest that mental processing, such as detecting the gaze direction or emotion of others, may not be a circumscribed cognitive process independent of executive domains. Yet, it may involve inhibition (i.e., delay of automatic responses) and may implicate allocation of attentional resource to non-PFC brain regions in HND. This study also showed that WM was associated with the number of functional connections to the right oSFG and that the emotion-recognition processing was associated with the degree of cluster

in the same region in HND, who also showed linear relationships within the EF domains. We suggest that the right oSFG could be a neural substrate candidate associated with integration in learning[46,47] and emotional mental processing[27] in OUD during abstinence. The data that explain our proposed hypothesis have yet to be obtained. Future prospective work identifying such relationship and utilizing a variety of ToM and EF subtests,[16] particularly during the protracted abstinent stage of the addiction cycle, is necessary to fully characterize our findings and would enhance our knowledge of the neuroadaptations underlying learning and planning and will shed light in interventional therapy.

4.1 Limitations and Future Prospectives

There are limitations in this study. This study suffers from relatively small sample sizes, due to insufficient grants and the enrollment of HND subjects that met criteria. Compensating for the limited sample sizes, we focused on controllable features (i.e., HND and ND with reduced variance), increased the size of observed effects (i.e., different parameters among groups), and provided visualization of the data. Although it may be way too far to provide generalization to the population, considering consistent hemodynamic patterns in the frontal area observed in another cohort in our previous work, this study may serve as an early guide for, and encourages, future large-scale translational investigations in various areas including, but not limited to, social cognition, identification of biomarkers, and development for brain state-dependent computation in OUD during recovery.

Like fMRI, fNIRS measures hemodynamic signals and solely relies on the principle of neurovascular transduction mechanism to construe neuronal event (i.e., blood flow). It relies on the ongoing spontaneous event to its applications in neuropharmacology to understand the physiological signals of the cerebral cortex. Despite its higher temporal resolution compared to fMRI, fNIRS can only monitor cortical activities. Thus, future prospective neuroimaging work is needed to explore the subcortical areas associated with the endocannabinoid, opioid, dopamine, and the aversive systems.

It bears mention that applying rsFC in the realm of OUD and linking FC with behaviors are still in their infant stages.[48,49] Prior studies have displayed inconsistent findings as a review[50] highlighted, and thus, their examinations, including this one, have been exploratory in nature. Both reduced[51,52] and enhanced[37,41,53] FC were reported in the PFC of opioid addicts. There have been only a few OUD studies in social cognition. Indeed, noninvasive neuroimaging measurements of spatiotemporal dynamics of network activity and neuropsychological assessment of cognition and behavior have been limited either by the accessibility of neuroimaging tools or by the consideration of the dynamics within the environment.[54] The inconsistency is probably due in large part to the associated comorbidity and handedness. Differentiation of comorbid phenotypes in accordance with subject cohorts, which may be a major factor accounting for the contrasting reports, is strongly recommended in future work. Utilizing noninvasive neuroimaging that owns high sensitivity and relatively high temporal and spatial resolutions at affordable cost will be optimal. Multimodal approaches will also be helpful in understanding brain network and its correlate with behavioral measures. It is worth noting that variables of circuit connectivity, thickness of cerebral cortex, and cognitive performance are often age-related; investigators should be cautious of the ages of the enrolled subjects and ensure that they are insignificant between study groups in future neuroimaging studies.

5 Conclusions

We present intrinsic differences in emotion recognition, EF, and PFC networks between HND and ND. These findings highlight distinct patterns in HND during recovery and may reflect potential neurobiological substrates, which may lead to identifying biomarker candidates for treatment. We hope that this pilot work adds to the literature by linking social cognition to brain functions and implicates in practices between clinician and OUD patient through gatekeeping strategies.

Appendix A: Supplementary Methods and Materials

A.1 Participants

One hundred and thirty individuals were recruited in this study between December 2015 and March 2016. There were two measuring sessions in the study. The first session was the neuropsychological measures that collected most of the behavioral data. The second session was the neuroimaging measures that collected the neurophysiological data. All subjects enrolled to the neuroimaging session were reminded to rest well the night before the experiment via phone calls. Five HND subjects could not participate in the neuroimaging session due to scheduling problems. Seven among the 110 C subjects were selected from the matched criteria with HND subjects for image acquisition (Fig. 1). Regular sleeping hours per day were self-reported during the neuropsychological assessment. The quality of sleep the night before was acquired before neuroimaging scanning, and the number of sleeping hours was recorded (Table 1) to eliminate possible confounders, such as insomnia. The HND and ND subjects were instructed to refrain from cigarette smoking during neuropsychological and neuroimaging measurements yet could smoke during breaks. All included HND and ND subjects smoked more than 16 cigarettes per day. The ND subjects were dependent on only nicotine during their lifetime. The HND subjects reported that they consumed other recreational substances in their lifetime but were not dependent on them. They reported that heroin had been their primary lifetime drug of dependence. Two HND subjects underwent methadone maintenance treatment. One HND individual was taking simvastatin (20 mg). One ND individual reported to take trazodone (50 mg) in lifetime but reported not taking during the period of the study.

A.2 Image Preprocessing and Analysis

All fNIRS data were preprocessed using software Homer2.[35] For the resting-state data, to generate relatively steady signals, the first 2-min measurements were excluded. The raw data were converted from optical density measurements to concentration changes in HbO based on the modified Beer–Lambert law.[1] The converted concentration signals were bandpass filtered (resting state: $0.01 < f_{rest} < 0.1$; task: $0.012 < f_{task} < 0.18$ in Hz). Detrending and motion correction using the spline interpolation and correlation-based signal improvement methods. Any data with low average signal intensity (>5 standard deviations) over time were considered poor quality and, thus, excluded from analyses. Detailed preprocessing procedures were discussed in our previous work.[2]

A.3 Functional Connectivity Network Analysis

For analyzing time courses of activation changes during RME task, mean levels of HbO signals during the first 20 s from the onset of stimulus, taking account for the 3-s mentalizing and the hemodynamic delay, were extracted and separated into bin data before network analysis. A single threshold presenting the absolute connectivity strength was chosen.

Both rsFC and graph-theory analyses could provide a comprehensive way to examine the network organizations between the study groups. Graph-theory analysis was then applied to

Table 7 Neuropsychological domains, functions, and tests administrated in this study.

Domain/function	Test
Executive functions (EF)	
Inhibition Inhibitory control and planning	Stroop test[9]
Shifting Abstraction, attention, and ability to shift cognitive strategies	Block design[10]
Updating Working memory	Working memory index Digit spin[10,11] Arithmetic[10]
Access Access to long-term memory, verbal, and spontaneous	Verbal fluency[12]
Processing speed Focused attention and automatic cognitive tasks	Processing speed subtests Symbol search[10] Coding[10]
Theory of mind (ToM)	
Emotion recognition Attribute of one's emotion, thought, and intention	Reading the mind in the eye[33] See Fig. 3
Clinical measures/behavioral stressors	
Childhood stress	Adverse childhood experiences questionnaire[14]
Depression	Beck depression inventory-II[15]
Anxiety	State-trait anxiety inventory[16]
Hyperactivity	Adult attention deficit/ hyperactivity disorder self-report (ASRS-v1.1) symptom checklist[17]

explore the resting-state network organization. A range of relative sparsity threshold from 0.05 to 0.6 (interval: 0.01) was applied. Six networks considered in this study properties: nodal degree strength, clustering coefficient, characteristic path length, small-worldness, nodal efficiency, and global efficiency, were examined to study the topological organizations. Using the software GRETNA,[3] the preprocessed data with N nodes were used to form an $N \times N$ correlation matrix, each presented the connectivity strength. Clustering coefficient of a given node (i.e., channel) and local efficiency are important measures of segregation among the node's neighboring topology. Path length and global efficiency are measures of integration in network analysis. Nodal degree is a measure of influence, quantifying the strength of a given edge.[4] The average graph property values over the sparsity range were further examined along with neuropsychological measures. We utilized methods described in detailed in our previous work. Group-level analyses were performed independently for each channel.

Prior neuroimaging has provided evidence that clustered patterns of intrinsic connectivity measured at rest could reflect cognitive functioning, such as behavioral control and intelligence.[5–7] To examine the link between rsFC network topological properties and behavioral performances, we performed correlation analyses of neural network topological properties and behavioral scores in EF, ToM, and clinical characteristics with the permutations tests. The method detail is available in the method of a recent study.[8]

Appendix B

The domains, functions and tasks in the neuropsychological battery in this study are in Table 7.

Appendix C

The MNI coordinates and their BA of the 14 channels are in Table 8.

Table 8 Channel coordinates were generated using NIRS-SPM software[34] after registration using a 3-D digitizer (Polhemus Inc., Vermont). Automated anatomical labeling (AAL) is applied.

ROI	Ch	Region (AAL)	Abbreviation	Coordinates (MNI)			Brodmann area (BA)
				x	y	z	
Right OFC	1	Right middle frontal gyrus, orbital part	oMFG_R	33	67	4	10/11
	4	Right superior frontal gyrus, orbital part	oSFG_R	22	72	6	10/11
	5	Right medial frontal gyrus	mOFC_R	9	74	7	10/11
Right dlPFC	2	Right middle frontal gyrus	MFG_R	44	52	26	46
	3	Right superior frontal gyrus	SFG_R	32	58	27	46
Right mPFC	6	Right superior frontal gyrus	SFG_R	19	65	29	10
	7	Right medial frontal gyrus	mPFC_R	10	67	29	10

Table 8 (*Continued*).

| ROI | Ch | Region (AAL) | Abbreviation | Coordinates (MNI) | | | Brodmann area (BA) |
				x	y	z	
Left mPFC	8	Left superior frontal gyrus, medial part	mSFG_L	−8	73	7	10/11
	9	Left superior frontal gyrus	SFG_L	−19	72	7	10/11
Left	12	Left superior frontal gyrus	SFG_L	−31	66	5	10/11
dlPFC	10	Left superior frontal gyrus	SFG_L	−7	66	30	10
Left OFC	11	Left superior frontal gyrus, medial part	mSFG_L	−18	65	27	10
	13	Left middle frontal gyrus	MFG_L	−29	59	26	46
	14	Left middle frontal gyrus	MFG_L	−39	53	25	46

References

1. B. Pajusco et al., "Tobacco addiction and smoking status in heroin addicts under methadone vs. buprenorphine therapy," *Int. J. Environ. Res. Public Health* **9**(3), 932–942 (2012).
2. R. A. Wise and G. F. Koob, "The development and maintenance of drug addiction," *Neuropsychopharmacology* **39**(2), 254–262 (2014).
3. G. F. Koob and E. J. Nestler, "The neurobiology of drug addiction," *J. Neuropsychiatry Clin. Neurosci.* **9**(3), 482–497 (1997).
4. E. J. Nestler, "Is there a common molecular pathway for addiction?" *Nat. Neurosci.* **8**(11), 1445–1449 (2005).
5. D. H. Malin et al., "The nicotinic antagonist mecamylamine precipitates nicotine abstinence syndrome in the rat," *Psychopharmacology* **115**(1), 180–184 (1994).
6. W. A. Corrigall et al., "The mesolimbic dopaminergic system is implicated in the reinforcing effects of nicotine," *Psychopharmacology* **107**(2), 285–289 (1992).
7. S. M. Trautmann and K. A. Sharkey, "Chapter Three—the endocannabinoid system and its role in regulating the intrinsic neural circuitry of the gastrointestinal tract," *Int. Rev. Neurobiol.* **125**, 85–126 (2015).
8. L. H. Parsons and Y. L. Hurd, "Endocannabinoid signaling in reward and addiction," *Nat. Rev. Neurosci.* **16**(10), 579–594 (2015).
9. R. Z. Goldstein et al., "Severity of neuropsychological impairment in cocaine and alcohol addiction: association with metabolism in the prefrontal cortex," *Neuropsychologia* **42**(11), 1447–1458 (2004).
10. D. Wechsler, "Wechsler adult intelligence scale–fourth edition (WAIS–IV)," (2014).
11. R. T. Lange, "Working Memory Index," *Encyclopedia of Clinical Neuropsychology*, J. S. Kreutzer, J. DeLuca, and B. Caplan, Eds., 2731–2732, Springer, New York (2011).
12. T. N. Tombaugh, J. Kozak, and L. Rees, "Normative data stratified by age and education for two measures of verbal fluency: FAS and animal naming," *Arch. of Clin. Neuropsychol.* **14**(2), 167–177 (1999).
13. S. Darke et al., "Comparative patterns of cognitive performance amongst opioid maintenance patients, abstinent opioid users and non-opioid users," *Drug Alcohol Depend.* **126**(3), 309–315 (2012).
14. J. A. Bargh, "Conditional automaticity: varieties of automatic influence in social perception and cognition," in *Unintended Thought*, J. S. Uleman and J. A. Bargh, Eds., Vol. **3**, pp. 51–69, Guilford Press, New York (1989).
15. C. D. Frith and T. Singer, "The role of social cognition in decision making," *Philos. Trans. R. Soc. B* **363**(1511), 3875–3886 (2008).
16. T. Aboulafia-Brakha et al., "Theory of mind tasks and executive functions: a systematic review of group studies in neurology," *J. Neuropsychol.* **5**(1), 39–55 (2011).
17. O. Sporns, "Structure and function of complex brain networks," *Dialogues Clin. Neurosci.* **15**(3), 247–262 (2013).
18. C. J. Evans and C. M. Cahill, "Neurobiology of opioid dependence in creating addiction vulnerability," *F1000Research* **5**, 1748 (2016).
19. F. A. Champagne and J. P. Curley, "How social experiences influence the brain," *Curr. Opin. Neurobiol.* **15**(6), 704–709 (2005).
20. M. A. Miller, A. K. Bershad, and H. de Wit, "Drug effects on responses to emotional facial expressions: recent findings," *Behav. Pharmacol.* **26**(6), 571–579 (2015).
21. C. Kornreich et al., "Impaired emotional facial expression recognition in alcoholics, opiate dependence subjects, methadone maintained subjects and mixed alcohol-opiate antecedents subjects compared with normal controls," *Psychiatry Res.* **119**(3), 251–260 (2003).
22. S. McDonald et al., "Deficits in social perception in opioid maintenance patients, abstinent opioid users and non-opioid users," *Addiction* **108**(3), 566–574 (2013).
23. M. Martin-Contero, R. Secades-Villa, and J. Tirapu-Ustarroz, "Social cognition in opiate addicts," *Rev. Neurol.* **55**(12), 705–712 (2012).
24. L. Martin et al., "Enhanced recognition of facial expressions of disgust in opiate users receiving maintenance treatment," *Addiction* **101**(11), 1598–1605 (2006).
25. B. Hanson et al., *Life with Heroin: Voices from the Inner City*, DC Heath, Lexington, Massachusetts (1985).
26. P. Bacchetti, S. G. Deeks, and J. M. McCune, "Breaking free of sample size dogma to perform innovative translational research," *Sci. Transl. Med.* **3**(87), 87ps24 (2011).
27. R. Saxe and L. J. Powell, "It's the thought that counts: specific brain regions for one component of theory of mind," *Psychol. Sci.* **17**(8), 692–699 (2006).
28. V. E. Stone, S. Baron-Cohen, and R. T. Knight, "Frontal lobe contributions to theory of mind," *J. Cognit. Neurosci.* **10**(5), 640–656 (1998).

29. A.-C. Ehlis et al., "Application of functional near-infrared spectroscopy in psychiatry," *NeuroImage* **85**, 478–488 (2014).
30. H. Obrig, "NIRS in clinical neurology—a 'promising' tool?" *NeuroImage* **85**, 535–546 (2014).
31. S. Baron-Cohen et al., "The 'Reading the Mind in the Eyes' test revised version: a study with normal adults, and adults with Asperger syndrome or high-functioning autism," *J. Child Psychol. Psychiatry* **42**(2), 241–251 (2001).
32. S. Baron-Cohen et al., "Social intelligence in the normal and autistic brain: an fMRI study," *Eur. J. Neurosci.* **11**(6), 1891–1898 (1999).
33. R. B. Adams, Jr. et al., "Cross-cultural Reading the Mind in the Eyes: an fMRI investigation," *J. Cognit. Neurosci.* **22**(1), 97–108 (2010).
34. J. C. Ye et al., "NIRS-SPM: statistical parametric mapping for near-infrared spectroscopy," *NeuroImage* **44**(2), 428–447 (2009).
35. C. M. Aasted et al., "Anatomical guidance for functional near-infrared spectroscopy: AtlasViewer tutorial," *Neurophotonics* **2**(2), 020801 (2015).
36. X. Cui et al., "A quantitative comparison of NIRS and fMRI across multiple cognitive tasks," *NeuroImage* **54**(4), 2808–2821 (2011).
37. H. F.-h. Ieong and Z. Yuan, "Abnormal resting-state functional connectivity in the orbitofrontal cortex of heroin users and its relationship with anxiety: a pilot fNIRS study," *Sci. Rep.* **7**, 46522 (2017).
38. H. Niu et al., "Revealing topological organization of human brain functional networks with resting-state functional near infrared spectroscopy," *PloS One* **7**(9), e45771 (2012).
39. P. Bacchetti, "Current sample size conventions: flaws, harms, and alternatives," *BMC Med.* **8**(1), 17 (2010).
40. N. Ma et al., "Addiction related alteration in resting-state brain connectivity," *NeuroImage* **49**(1), 738–744 (2010).
41. J. Liu et al., "Dysfunctional connectivity patterns in chronic heroin users: an fMRI study," *Neurosci. Lett.* **460**(1), 72–77 (2009).
42. D. P. Chapman et al., "Adverse childhood experiences and the risk of depressive disorders in adulthood," *J. Affective Disord.* **82**(2), 217–225 (2004).
43. G. F. Koob and N. D. Volkow, "Neurocircuitry of addiction," *Neuropsychopharmacology* **35**(1), 217–238 (2010).
44. K. Yuan et al., "Combining spatial and temporal information to explore resting-state networks changes in abstinent heroin-dependent individuals," *Neurosci. Lett.* **475**(1), 20–24 (2010).
45. J. Le Merrer et al., "Reward processing by the opioid system in the brain," *Physiol. Rev.* **89**(4), 1379–1412 (2009).
46. K. Christoff et al., "Rostrolateral prefrontal cortex involvement in relational integration during reasoning," *NeuroImage* **14**(5), 1136–1149 (2001).
47. C. Wendelken and S. A. Bunge, "Transitive inference: distinct contributions of rostrolateral prefrontal cortex and the hippocampus," *J. Cognitive Neurosci.* **22**(5), 837–847 (2010).
48. H. Lu and E. A. Stein, "Resting state functional connectivity: its physiological basis and application in neuropharmacology," *Neuropharmacology* **84**, 79–89 (2014).
49. R. Z. Goldstein and N. D. Volkow, "Dysfunction of the prefrontal cortex in addiction: neuroimaging findings and clinical implications," *Nat. Rev. Neurosci.* **12**(11), 652–669 (2011).
50. M. T. Sutherland et al., "Resting state functional connectivity in addiction: lessons learned and a road ahead," *NeuroImage* **62**(4), 2281–2295 (2012).
51. P.-W. Wang et al., "Abnormal interhemispheric resting state functional connectivity of the insula in heroin users under methadone maintenance treatment," *Psychiatry Res. Neuroimaging* **255**, 9–14 (2016).
52. J. Upadhyay et al., "Alterations in brain structure and functional connectivity in prescription opioid-dependent patients," *Brain* **133**(7), 2098–2114 (2010).
53. S. J. Russo et al., "The addicted synapse: mechanisms of synaptic and structural plasticity in nucleus accumbens," *Trends Neurosci.* **33**(6), 267–276 (2010).
54. A. Bandura, "A sociocognitive analysis of substance abuse: an agentic perspective," *Psychol. Sci.* **10**(3), 214–217 (1999).

Hada Fong-ha Ieong studied forensic science with minors in biology and chemistry at Seattle University before receiving her MS degree in forensic toxicology from the University of Florida. She is completing her PhD in biomedical sciences at the University of Macau and is pursuing a medical carreer. Her research focuses on understanding the neuropathology of opiate addiction through neuroimaging and neuropsychological techniques.

Zhen Yuan is the director of the Bioimaing Core and a tenured associate professor at the Faculty of Health Sciences, the University of Macau. He received his PhD in mechanical engineering at the University of Sciences and Technology of China. His research focuses on developing innovative multimodal imaging techniques to study biological systems and materials. He is also a senior member of the Optical Society (OSA) and SPIE.